

Supporting information:

Ultra small subnano TiO_x cluster as an excellent co-catalyst for photocatalytic degradation of tetracycline on plasmonic Ag/AgCl

Wenlu He,^a Kaiwen Wang,^b Zhu Zhu,^b Hanjun Zou,^c Kai Zhou,^c Zhao Hu,^d Youyu Duan,^a Yajie Feng,^a Liyong Gan,^a Kangle Lv,^d Cong Wang,^{*b} Xiaodong Han,^{*b} and Xiaoyuan Zhou^{*a,c}

^[a]College of Physics, Chongqing University, Chongqing 401331, P. R. China

^[b]Beijing Key Laboratory and Institute of Microstructure and Property of Advanced Materials, Beijing University of Technology, Beijing 100124, P. R. China

^[c] Analytical and Testing Center, Chongqing University, Chongqing 401331, P. R. China

^[d] College of Resources and Environmental Science, South-Central University for Nationalities, Wuhan 430074, P. R. China

*Corresponding authors Emails:

smartswang@bjut.edu.cn (C. W); xdhan@bjut.edu.cn (X. H); xiaoyuan2013@cqu.edu.cn (X. Z).

This file includes:

Fig. S1 (a) XRD patterns of TiO_x@Ag/AgCl loaded with different concentrations of TiO_x from 0.1 to 5 times of the as-prepared fresh sample and the pristine sample; (b) XRD patterns of the as-prepared fresh TiO_x@Ag/AgCl and the used TiO_x@AgCl after 10 cycles.

Fig. S2 PL spectra of the as-prepared TiO_x@Ag/AgCl, 0.1TiO_x@Ag/AgCl and the synthesized Ag/AgCl.

Fig. S3. FTIR spectra of the as-prepared TiO_x@Ag/AgCl and the synthesized Ag/AgCl

Fig. S4 EIS nyquist plots of Ag/AgCl and TiO_x@Ag/AgCl

Fig. S5 Absorption spectrums of the degradation of TC with the presence of $\text{TiO}_x@Ag/AgCl$.

Fig. S6 Dependence of the TC adsorption efficiency on the $\text{TiO}_x@Ag/AgCl$ in the dark

Fig. S7 HAADF images of $\text{TiO}_x@Ag/AgCl$ exposed under different time of electron beam irradiation a) 0 s; b) 10 s; c) 20 s; d) 30 s; e) 40 s; f) 50 s.

Fig. S8 Effect of different scavengers on photocatalytic degradation

Fig. S9. Effect of different scavengers on photocatalytic degradation ESR signals of $\text{DMPO-O}_2\cdot^-$ and $\text{DMPO-HO}\cdot$ of $\text{TiO}_x@Ag/AgCl$. scavengers on photocatalytic degradation.

Fig. S10. LC-MS analysis of TC and its intermediates in the photodegradation reaction

Fig. S11. Proposed possible pathways of photocatalytic degradation of TC

Table. S1 EDX result of $\text{TiO}_x@Ag/AgCl$

Table. S2 Corresponding reaction rate constant k of TC of various catalyst

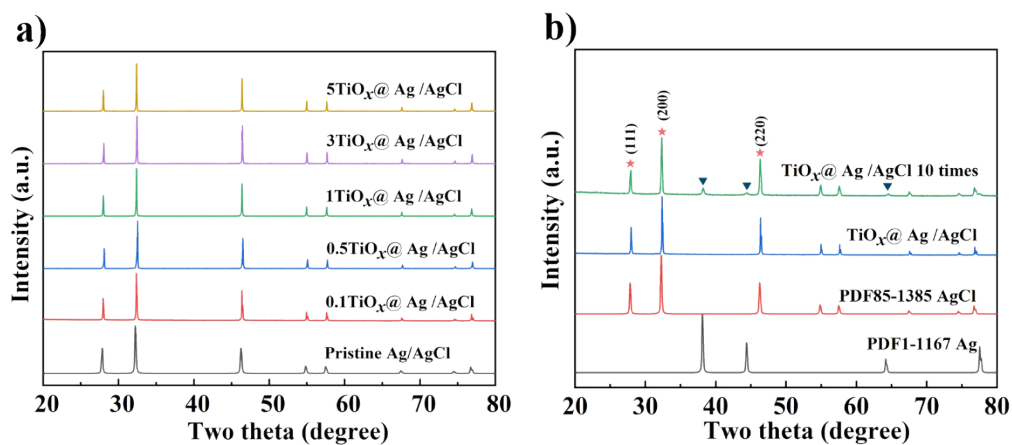


Fig. S1. (a) XRD patterns of $\text{TiO}_x@ \text{Ag} / \text{AgCl}$ loaded with different concentrations of TiO_x from 0.1 to 5 times of the as-prepared fresh sample and the pristine sample. (b) XRD patterns of the as-prepared fresh $\text{TiO}_x@ \text{Ag} / \text{AgCl}$ and the used $\text{TiO}_x@ \text{Ag} / \text{AgCl}$ after 10 cycles.

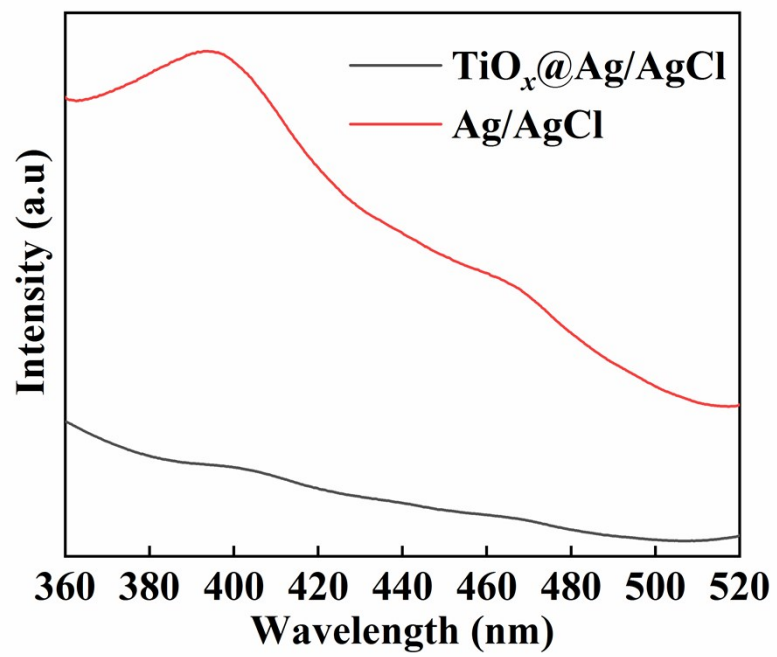


Fig. S2. PL spectra of $\text{TiO}_x@Ag/AgCl$ and the synthesized $Ag/AgCl$.

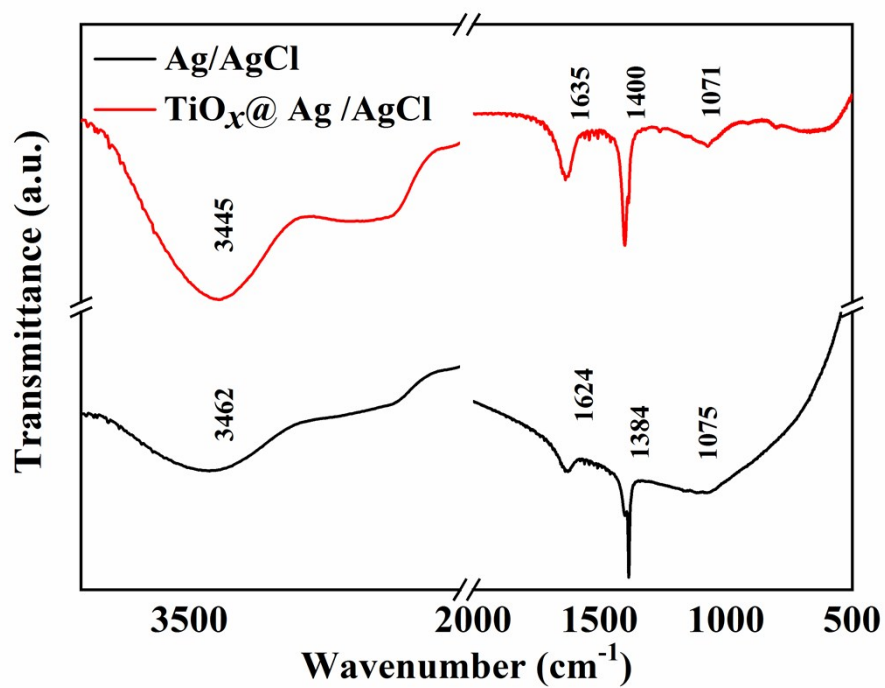


Fig. S3. FTIR spectra of the as-prepared TiO_x@Ag/AgCl and the synthesized Ag/AgCl.

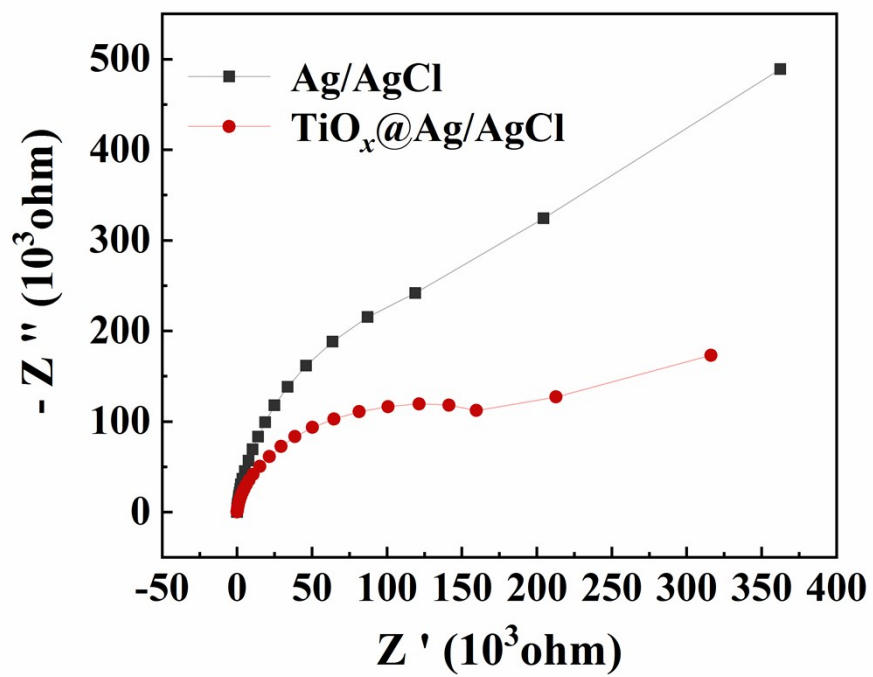


Fig. S4. EIS nyquist plots of Ag/AgCl and $\text{TiO}_x@Ag/AgCl$ in 0.5 M Na_2SO_4 aqueous solution in the dark.

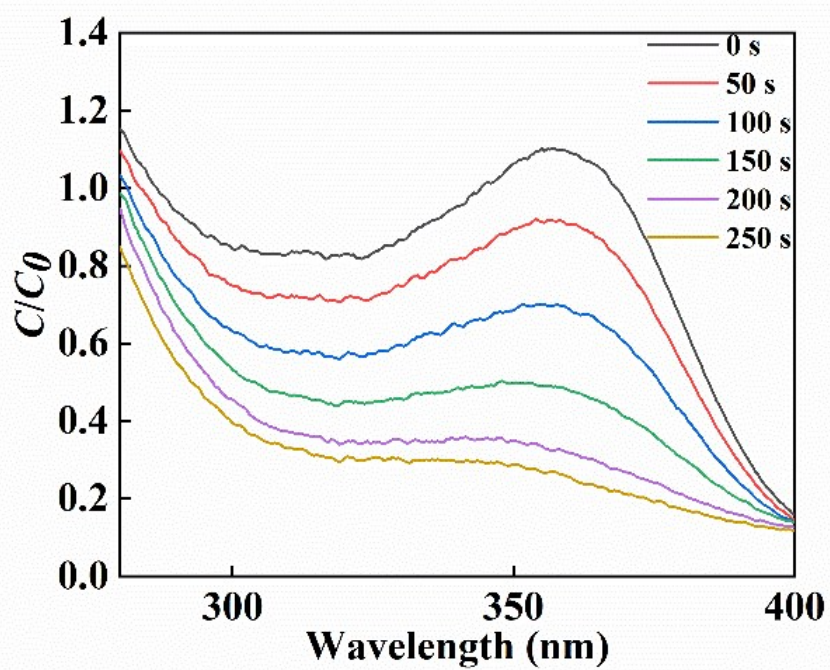


Fig. S5. Absorption spectrums of the degradation of TC with the presence of $\text{TiO}_x@Ag/AgCl$.

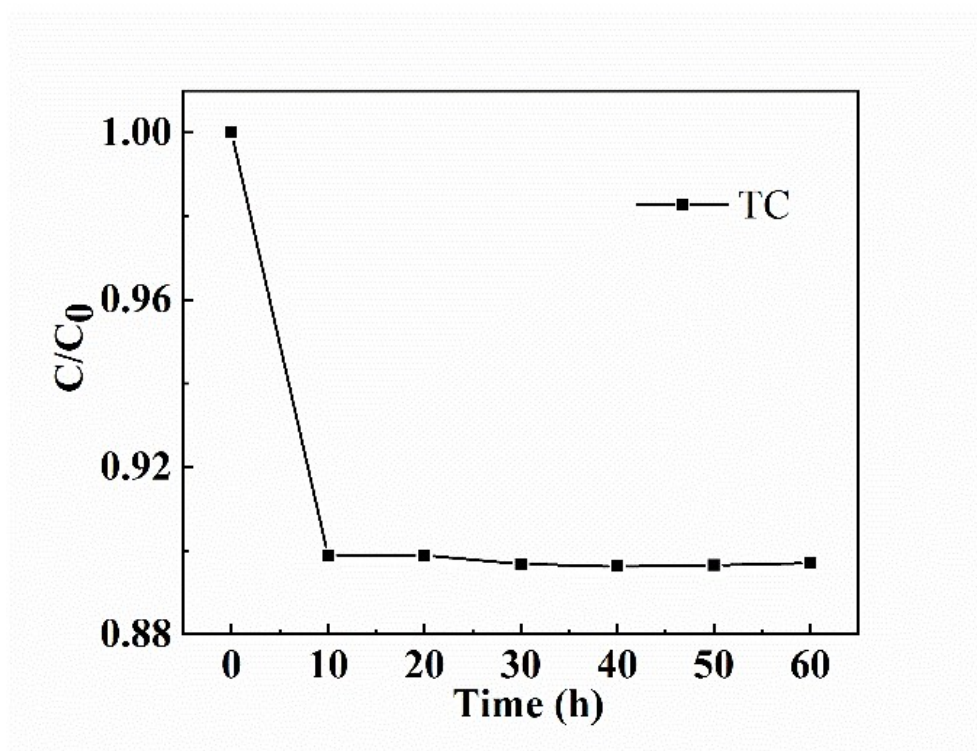


Fig. S6. Dependence of the TC adsorption efficiency on the $\text{TiO}_x@Ag/AgCl$ in the dark

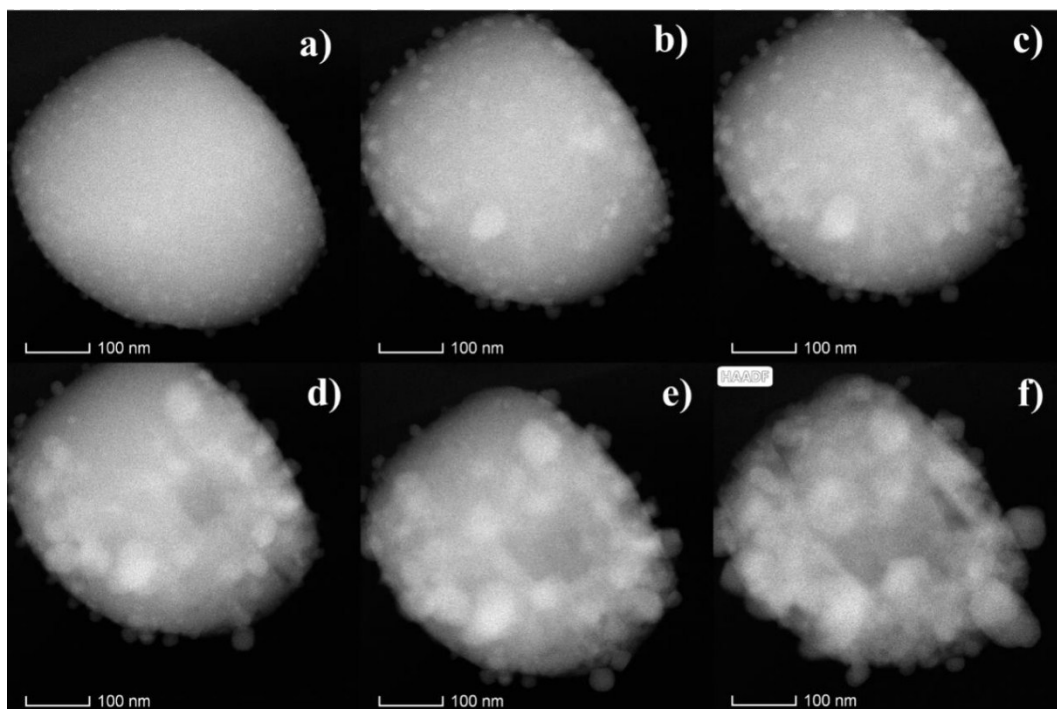


Fig. S7. HAADF images of $\text{TiO}_x@Ag/AgCl$ exposed under different time of electron beam irradiation a) 0 s; b) 10 s; c) 20 s; d) 30 s; e) 40 s; f) 50 s.

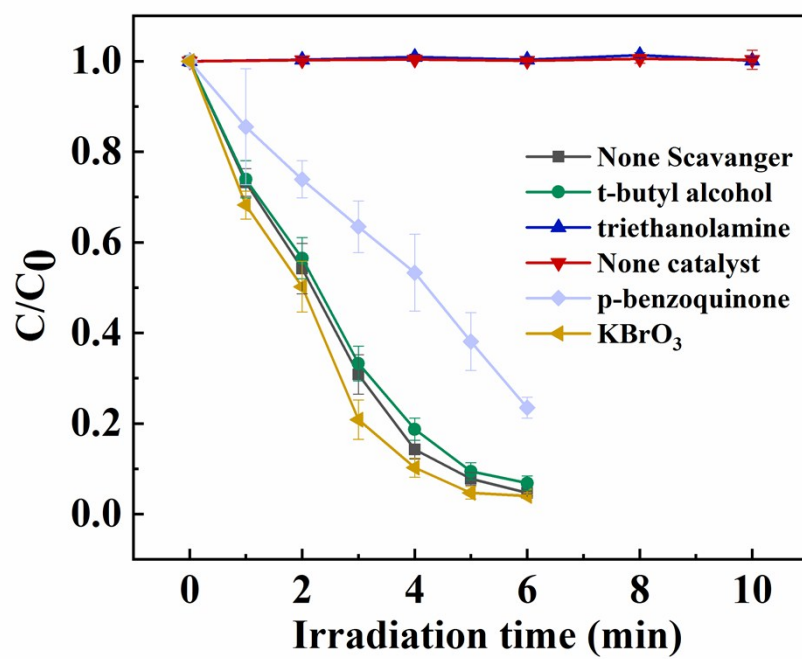


Fig. S8. Effect of different scavengers on photocatalytic degradation.

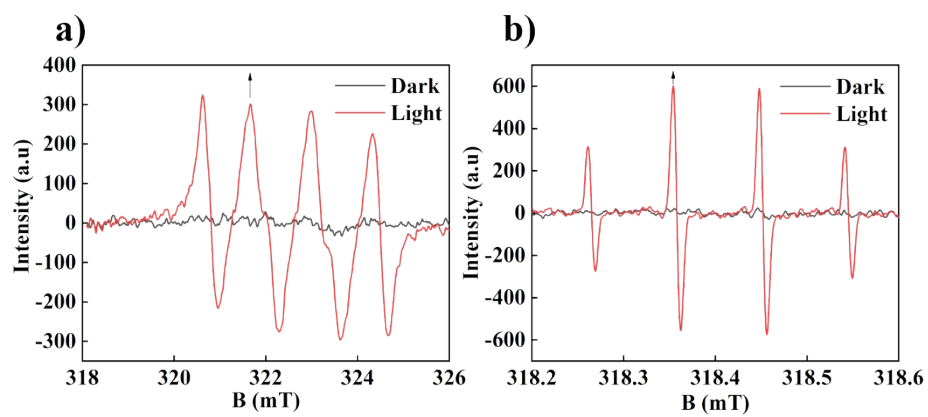


Fig. S9. ESR signals of DMPO-O₂•⁻ and DMPO-HO• of TiO_x@Ag/AgCl.

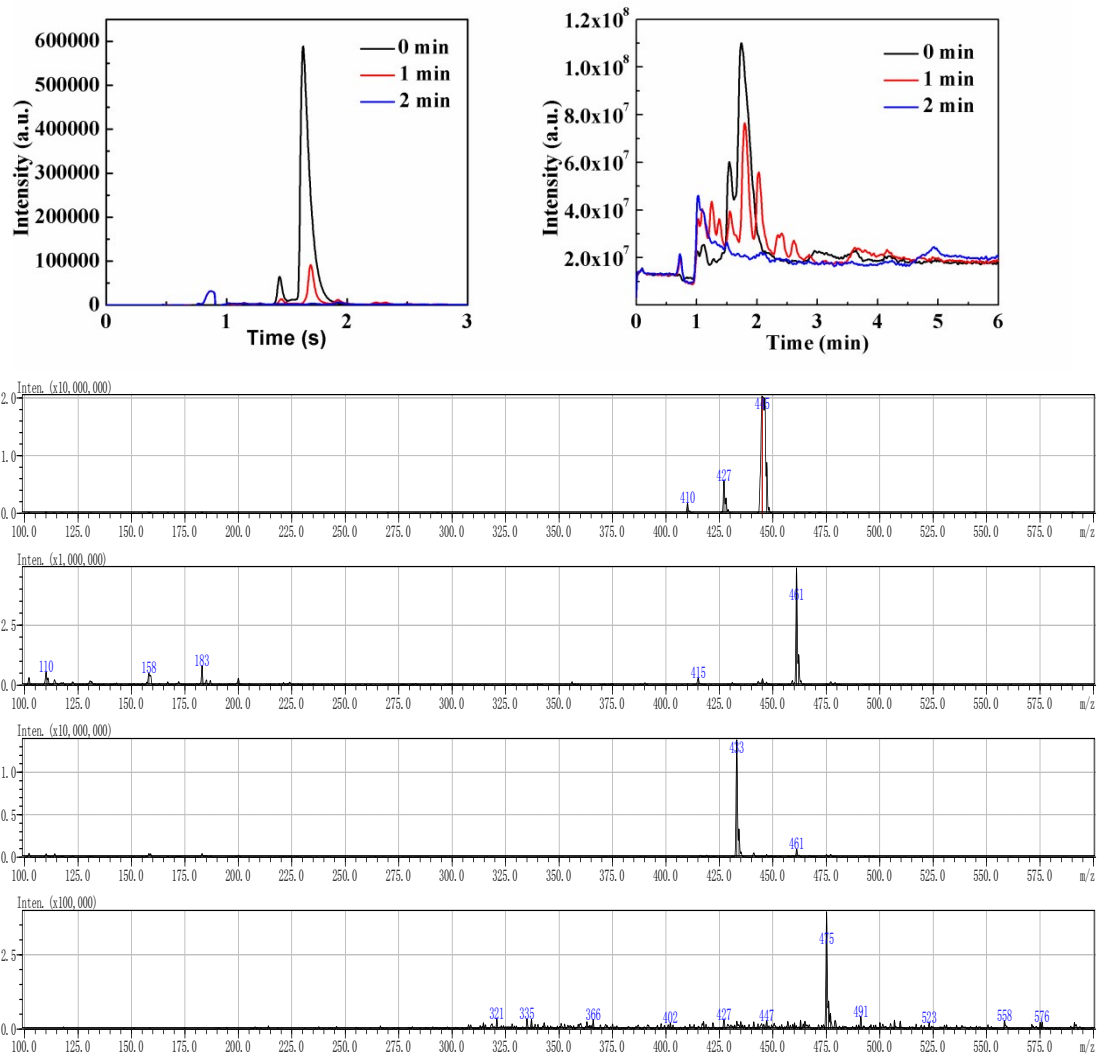


Fig. S10. LC-MS analysis of TC and its intermediates in the photodegradation reaction

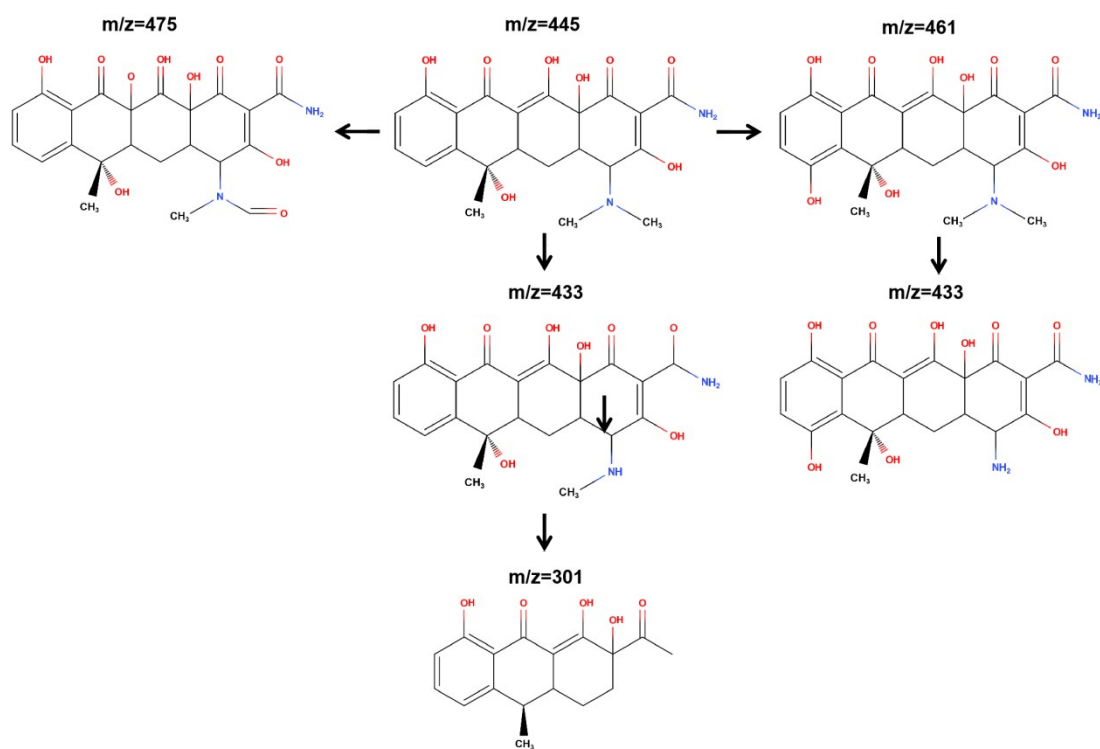


Fig. S11. Proposed possible pathways of photocatalytic degradation of TC

Table S1 EDX result of TiO_x@Ag/AgCl

Element	Atomic Fraction (%)	Mass Fraction (%)
Ag (L)	49.51	24.89
Cl (K)	50.09	0.27
Ti (K)	0.41	74.84

Table S2 Corresponding reaction rate constant (k) of TC and MO of various catalyst

Material structure	Light source	Light condition	Organic pollutants	Degradation rate
TiOx@Ag/AgCl (This work)	300 W Xe lamp	AM 1.5G	tetracycline	0.49247 min ⁻¹
N-doped BiOIO ₃ ¹	LED light	357 nm	tetracycline	0.04025 min ⁻¹
BiVO ₄ (0 4 0)-Ag@CdS ²	300W Xe lamp	≥420 nm	tetracycline	0.0875 min ⁻¹
Cu/Cl-g-C ₃ N ₄ ³	300W Xe lamp	≥400 nm	tetracycline	0.0271 min ⁻¹
AgI/Bi ₂ WO ₆ ⁴	300W Xe lamp	≥420 nm	tetracycline	0.075 min ⁻¹
CoO/g-C ₃ N ₄ ⁵	300W Xe lamp	≥400 nm	tetracycline	0.0173 min ⁻¹
LDH-Ag ₂ O/Ag ⁶	300W Xe lamp	≥420 nm	tetracycline	0.0184 min ⁻¹
α-Fe ₂ O ₃ @g-C ₃ N ₄ ⁷	100W LED lamp	420 nm	tetracycline	0.042 min ⁻¹
Fe-doped surface-alkalinized g-C ₃ N ₄ ⁸	300W Xe lamp	≥420 nm	tetracycline	0.0164 min ⁻¹
Nitrogen modified titania /strontium ferrite/diatomite (N-TSD) ⁹	150W Xe lamp	≥400 nm	tetracycline	0.0165 min ⁻¹
Bi ₂ WO ₆ /CuBi ₂ O ₄ ¹⁰	300W Xe lamp	≥400 nm	tetracycline	0.0393 min ⁻¹
NiFe ₂ O ₄ /C yolk-shell nanospheres ¹¹	800W Xe lamp	≥420 nm	tetracycline	0.44295 min ⁻¹
CQDs/ZnO@HNTs ¹²	500W Xe lamp	≥420 nm	tetracycline	0.0275 min ⁻¹
carbon-doped Bi ₂ MoO ₆ ¹³	300W Xe lamp	≥420 nm	tetracycline	0.0399 min ⁻¹
(Mo,C)-TiO ₂ /FTO ¹⁴	500W Xe lamp	≥420 nm	tetracycline	0.0221 min ⁻¹
Poly (triazine imide) hollow tube (PTI)/ZnO heterojunction ¹⁵	300W Xe lamp	≥420 nm	tetracycline	0.034 min ⁻¹
CNT/LaVO ₄ ¹⁶	300W Xe lamp	≥420 nm	tetracycline	0.0098 min ⁻¹
Bi ₂ S ₃ @Bi ₂ WO ₆ /WO ₃ ¹⁷	400W Xe lamp	≥420 nm	tetracycline	0.0168 min ⁻¹

Bi-CNNS ¹⁸	300W Xe lamp	≥420 nm	tetracycline	0.09458 min ⁻¹
PoPD/AgCl-35/CN ¹⁹	250W Xe lamp	≥420 nm	tetracycline	0.0375 min ⁻¹
MCU-C ₃ N ₄ ²⁰	300W Xe lamp	≥420 nm	tetracycline	0.022 min ⁻¹
WO ₃ /Bi ₁₂ O ₁₇ Cl ₂ ²¹	300W Xe lamp	≥420 nm	tetracycline	0.0046 min ⁻¹
QDs/BiOCl/BiOBr ²²	250W Xe lamp	≥400 nm	tetracycline	0.0133 min ⁻¹
Bi ₂ MoO ₆ /NiTiO ₃ ²³	300W Xe lamp	≥400 nm	tetracycline	0.0243 min ⁻¹
BiVO ₄ /N-CQDs/Ag ₃ PO ₄ ²⁴	300W Xe lamp	≥420 nm	tetracycline	0.07097 min ⁻¹
Bi ₂ Zr ₂ O ₇ ²⁵	Xe lamp	Simulated sunlight	tetracycline	0.00868 min ⁻¹
Eu-CN@BiVO ₄ ²⁶	300W Xe lamp	≥420 nm	tetracycline	0.06528 min ⁻¹
Ag ⁰ (NP)/TiO ₂ ²⁷	UV-A lamp	= 360 nm	tetracycline	0.0112 min ⁻¹
C-doped TiO ₂ ²⁸	25W flexible white visLED light	= 450 nm	tetracycline	0.0099 min ⁻¹
NiS and MoS ₂ nanosheet comodified graphitic C ₃ N ₄ ²⁹	Xe lamp	≥400 nm	tetracycline	0.0254 min ⁻¹
AgBr/CuBi ₂ O ₄ ³⁰	300W Xe lamp	≥420 nm	tetracycline	0.03511 min ⁻¹
FeNi ₃ /SiO ₂ /CuS ³¹	18W UV lamp	= 254 nm	tetracycline	0.0257 min ⁻¹
α-Bi ₂ O ₃ /g-C ₃ N ₄ ³²	300W Xe lamp	≥400 nm	tetracycline	0.01223 min ⁻¹
β-Bi ₂ O ₃ @g-C ₃ N ₄ ³³	250W Xe lamp	≥420 nm	tetracycline	0.0311 min ⁻¹
CdS/SnO ₂ ³⁴	300W Xe lamp	≥420 nm	tetracycline	0.0143 min ⁻¹
CdS/Bi ₃ O ₄ Cl ³⁴	250W Xe lamp	≥420 nm	tetracycline	0.0643 min ⁻¹
BiOBr/CTF-3D ³⁵	500W Xe lamp	≥420 nm	tetracycline	0.04122 min ⁻¹

RGO-ZnTe ³⁶	solar simulator	AM 1.5G	tetracycline	0.033 min ⁻¹
potassium (K)-doped porous ultrathin g-C ₃ N ₄ ³⁷	300W Xe lamp	≥300 nm	tetracycline	0.0282 min ⁻¹
In ₂ S ₃ /BiPO ₄ ³⁸	350W Xe lamp	≥400 nm	tetracycline	0.0145 min ⁻¹
carbon dots/NiCo ₂ O ₄ ³⁹	300W Xe lamp	≥420 nm	tetracycline	0.02134 min ⁻¹
In ₂ O ₃ ³⁹	250W Xe lamp	≥420 nm	tetracycline	0.0073 min ⁻¹
Bi ₂ WO ₆ /Ag ₂ O/CQDs ⁴⁰	500W Xe lamp	≥400 nm	tetracycline	0.035 min ⁻¹

References

- [1] L. Huang, Y. Wang, Y. Li, S. Huang, Y. Xu, H. Xu, H. Li, *Materials Letters*, **2019**, 246,219-222.
- [2] Y. Xue, Z. Wu, X. He, Q. Li, X. Yang, L. Li, *Journal of Colloid Interface Science*, **2019**, 548,293-302.
- [3] C. Li, S. Yu, X. Zhang, Y. Wang, C. Liu, G. Chen, H. Dong, *Journal of Colloid Interface Science*, **2019**, 538,462-473.
- [4] W. Xue, Z. Peng, D. Huang, G. Zeng, X. Wen, R. Deng, Y. Yang, X. Yan, *Ceramics International*, **2019**, 45,6340-6349.
- [5] J. Niu, Y. Xie, H. Luo, Q. Wang, Y. Zhang, Y. Wang, *Chemosphere*, **2019**, 218,169-178.
- [6] C.R. Chen, H.Y. Zeng, M.Y. Yi, G.F. Xiao, R.L. Zhu, X.J. Cao, S.G. Shen, J.W. Peng, *Ecotoxicology and Environmental Safety*, **2019**, 172,423-431.
- [7] T. Guo, K. Wang, G. Zhang, X. Wu, *Applied Surface Science*, **2019**, 469,331-339.
- [8] Y. Xu, F. Ge, Z. Chen, S. Huang, W. Wei, M. Xie, H. Xu, H. Li, *Applied Surface Science*, **2019**, 469, 739-746.
- [9] Q. Wu, Z. Zhang, *International Journal of Hydrogen Energy*, **2019**, 44,8261-8272.
- [10] X. Yuan, D. Shen, Q. Zhang, H. Zou, Z. Liu, F. Peng, *Chemical Engineering Journal*, **2019**, 369,292-301.
- [11] Z. Chen, Y. Gao, D. Mu, H. Shi, D. Lou, S.Y. Liu, *Dalton Trans*, **2019**, 48,3038-3044.
- [12] J. Li, K. Liu, J. Xue, G. Xue, X. Sheng, H. Wang, P. Huo, Y. Yan, *Journal of Catalysis*, **2019**, 369,450-461.
- [13] Y. Xing, X. Gao, G. Ji, Z. Liu, C. Du, *Applied Surface Science*, **2019**, 465,369-382.
- [14] X. Niu, W. Yan, C. Shao, H. Zhao, J. Yang, *Applied Surface Science*, **2019**, 466, 882-892.
- [15] X. Yan, J. Qin, G. Ning, J. Li, T. Ai, X. Su, Z. Wang, *Advanced Powder Technology*, **2019**, 30,359-365.
- [16] Y. Xu, J. Liu, M. Xie, L. Jing, H. Xu, X. She, H. Li, J. Xie, *Chemical Engineering Journal*, **2019**, 357,487497.
- [17] H. Liu, H. Zhou, H. Li, X. Liu, C. Ren, Y. Liu, W. Li, M. Zhang, *Journal of the Taiwan Institute of Chemical Engineers*, **2019**, 95, 94-102.
- [18] M. Wang, C. Jin, Z. Li, M. You, Y. Zhang, T. Zhu, *Journal of Colloid Interface Science*, **2019**, 533,513-525.
- [19] L. Sun, C. Liu, J. Li, Y. Zhou, H. Wang, P. Huo, C. Ma, Y. Yan, *Chinese Journal of Catalysis*, **2019**, 40,80-94.
- [20] Y. Shi, J. Huang, G. Zeng, W. Cheng, H. Yu, Y. Gu, L. Shi, K. Yi, Stable, metal-free, *Journal of Colloid Interface Science*, **2018**, 531,433-443.
- [21] J. Zheng, F. Chang, M. Jiao, Q. Xu, B. Deng, X. Hu, *Journal of Colloid Interface Science*, **2018**, 510,20-31.
- [22] Q. Hu, M. Ji, J. Di, B. Wang, J. Xia, Y. Zhao, H. Li, *Journal of Colloid Interface Science*, **2018**, 519,263-272.
- [23] S. Li, S. Hu, W. Jiang, Y. Liu, Y. Zhou, Y. Liu, L. Mo, *Journal of Colloid Interface Science*, **2018**, 521, 42-49.
- [24] J. Zhang, M. Yan, X. Yuan, M. Si, L. Jiang, Z. Wu, H. Wang, G. Zeng, *Journal of Colloid Interface Science*, **2018**, 529,11-22.
- [25] X. Liu, L. Huang, X. Wu, Z. Wang, G. Dong, C. Wang, Y. Liu, L. Wang, *Chemosphere*, **2018**, 210,424-432.
- [26] M. Wang, P. Guo, Y. Zhang, T. Liu, S. Li, Y. Xie, Y. Wang, T. Zhu, *Applied Surface Science*, **2018**, 453, 11-22.

- [27] A. Tiwari, A. Shukla, Lalliansanga, D. Tiwari, S.M. Lee, *Journal of Environmental Management*, **2018**, 220,96-108.
- [28] E.O. Oseghe, A.E. Ofomaja, *Journal of Environmental Management*, **2018**, 223,860-867.
- [29] X. Lu, Y. Wang, X. Zhang, G. Xu, D. Wang, J. Lv, Z. Zheng, Y. Wu, *Journal of Hazard Materials*, **2018**, 341,10-19.
- [30] F. Guo, W. Shi, H. Wang, M. Han, W. Guan, H. Huang, Y. Liu, Z. Kang, *Journal of Hazard Materials*, **2018**, 349,111-118.
- [31] N. Nasseh, L. Taghavi, B. Barikbin, M.A. Nasser, *Journal of Cleaner Production*, **2018**, 179,42-54.
- [32] D. Chen, S. Wu, J. Fang, S. Lu, G. Zhou, W. Feng, F. Yang, Y. Chen, Z. Fang, *Separation and Purification Technology*, **2018**, 193, 232-241.
- [33] Y. Hong, C. Li, B. Yin, D. Li, Z. Zhang, B. Mao, W. Fan, W. Gu, W. Shi, *Chemical Engineering Journal*, **2018**, 338, 137-146.
- [34] L. Zhang, C.-G. Niu, C. Liang, X.-J. Wen, D.-W. Huang, H. Guo, X.-F. Zhao, G.-M. Zeng, *Chemical Engineering Journal*, **2018**, 352, 863-875.
- [35] S.-R. Zhu, Q. Qi, Y. Fang, W.-N. Zhao, M.-K. Wu, L. Han, *Crystal Growth & Design*, **2017**, 18, 883-891.
- [36] K. Chakraborty, T. Pal, S. Ghosh, *ACS Applied Nano Materials*, **2018**, 1, 3137-3144.
- [37] W. Wang, P. Xu, M. Chen, G. Zeng, C. Zhang, C. Zhou, Y. Yang, D. Huang, C. Lai, M. Cheng, L. Hu, W. Xiong, H. Guo, M. Zhou, *ACS Sustainable Chemistry & Engineering*, **2018**, 6, 15503-15516.
- [38] M. Zhang, Z. Hou, W. Ma, X. Zhao, C. Ma, Z. Zhu, Y. Yan, C. Li, *New Journal of Chemistry*, **2018**, 42, 15136-15145.
- [39] J. Jiang, W. Shi, F. Guo, S. Yuan, *Inorganic Chemistry Frontiers*, **2018**, 5, 1438-1444.
- [40] J. Shen, J. Xue, G. He, J. Ni, Z. Chen, B. Tang, Z. Zhou, H. Chen, *Journal of Materials Science*, **2018**, 53, 12040-12055.